Materials Today Bio 28 (2024) 101177

Contents lists available at ScienceDirect

Materials Today Bio

journal homepage: www.journals.elsevier.com/materials-today-bio

Curcumin loaded hydrogel with double ROS-scavenging effect regulates microglia polarization to promote poststroke rehabilitation

Shulei Zhang [a,1], Yuanyuan Ran [b,1], Yerasel Tuolhen [a], Yufei Wang [a], Guiqin Tian [b], Jianing Xi [b], Zengguo Feng [a], Wei Su [c,**], Lin Ye [a,d,*], Zongjian Liu [b,***]

[a] School of Materials Science and Engineering, Beijing Institute of Technology, Beijing, 100081, China
[b] Beijing Rehabilitation Hospital, Capital Medical University, Beijing, 100144, China
[c] Beijing Tsinghua Chang Gung Hospital, School of Clinical Medicine, Tsinghua University, Beijing, 102218, China
[d] Tangshan Research Institute, Beijing Institute of Technology, Tangshan, 063000, China

ARTICLE INFO

Keywords:
ROS scavenge
Stroke
Injectable hydrogel
Microglia
Anti-inflammatory phenotype
Curcumin

ABSTRACT

Cyclodextrins are used to include curcumin to form complex, which is subsequently loaded into a reactive oxygen species (ROS) responsive hydrogel (Cur gel). This gel exhibits a dual ROS scavenging effect. The gel can neutralize extracellular ROS to lead to a ROS-sensitive curcumin release. The released curcumin complex can eliminate intracellular ROS. Furthermore, the Cur gel effectively downregulates the expression of CD16 and IL-1β while upregulating CD206 and TGF-β in oxygen and glucose-deprived (OGD) BV2 cells. Additionally, it restores the expression of synaptophysin and PSD95 in OGD N2a cells. Upon injection into the stroke cavity, the Cur gel reduces CD16 expression and increases CD206 expression in the peri-infarct area of stroke mice, indicating an *in vivo* anti-inflammatory polarization of microglia. Colocalization studies using PSD95 and VGlut-1 stains, along with Golgi staining, reveal enhanced neuroplasticity. As a result, stroke mice treated with the Cur gel exhibit the most significant motor function recovery. Mechanistic investigations demonstrate that the released curcumin complex scavenges ROS and suppresses the activation of the ROS-NF-κB signaling pathway by inhibiting the translocation of p47-*phox* and p67-*phox* to lead to anti-inflammatory microglia polarization. Consequently, the Cur gel exhibits promising potential for promoting post-stroke rehabilitation in clinics.

1. Introduction

Stroke stands as the second leading cause of mortality and disability worldwide [1,2]. Given the narrow window for effective clinical therapy, over 75 % of patients necessitate poststroke rehabilitation. However, Current clinical rehabilitation methods are far from satisfactory [3]. Therefore, there is a pressing need for a novel clinical rehabilitation treatment that transcends the constraints of traditional poststroke rehabilitation. Recent advancements in cell, drug, and gene therapy have shown promising results in promoting poststroke rehabilitation [4–6]. Our investigations have delved into the roles of various drugs, including curcumin [7], melatonin [8], candesartan [9], baicalein [10], and bio-drugs such as tannic acid [11], brain-derived neurotrophic factor (BDNF), and vascular endothelial growth factor (VEGF) [12]. These studies, conducted during the subacute/chronic phases after a stroke, have demonstrated their efficacy in enhancing neuroplasticity by modulating microglial polarization toward an anti-inflammatory phenotype. Consequently, we propose a novel and feasible strategy for poststroke rehabilitation, focusing on enhancing neuroplasticity through the regulation of microglial polarization [13–16].

Microglia, as resident immune cells in the central nervous system, are primarily tasked with maintaining normal immune homeostasis. Following a stroke, microglia undergo activation and dynamic polarization, shifting from a beneficial anti-inflammatory phenotype to a neurotoxic proinflammatory phenotype. This transformation involves morphological and functional changes that negatively impact neuroplasticity, including synaptic remodeling, axonal sprouting, and dendritic spine regeneration. One of the most hazardous substances secreted

* Corresponding author. School of Materials Science and Engineering, Beijing Institute of Technology, Beijing, 100081, China.
** Corresponding author.
*** Corresponding author.
E-mail addresses: swa01179@btch.edu.cn (W. Su), yelin@bit.edu.cn (L. Ye), liuzj888@ccmu.edu.cn (Z. Liu).
[1] These authors contributed equally.

https://doi.org/10.1016/j.mtbio.2024.101177
Received 3 May 2024; Received in revised form 1 July 2024; Accepted 1 August 2024
Available online 2 August 2024

by proinflammatory microglia is reactive oxygen species (ROS). The accumulation of ROS in the brain creates a toxic environment for neighboring neurons, hindering the integration of newly formed neurons, impeding axon development [17], and resulting in functional deficits [18]. Proliferation of ROS also induces oxidative stress injury, activating and aggregating microglia, stimulating the secretion of inflammatory factors, and exacerbating the inflammatory response. Consequently, it becomes crucial to reduce ROS levels and promote nerve regeneration and functional recovery during poststroke rehabilitation [19]. Conversely, the anti-inflammatory phenotype assumes a distinct role compared to proinflammatory microglia in poststroke rehabilitation. This phenotype has been reported to produce neuroprotective factors that enhance synaptic plasticity and promote functional outcomes following a stroke. As a result, strategies focused on scavenging ROS and inducing anti-inflammatory microglial polarization have emerged as potential rehabilitative approaches to restore neurofunction after a stroke.

Curcumin (Cur) is a naturally occurring anti-inflammatory compound found in turmeric (Curcuma longa), associated with the inhibition of NF-κB, regulation of apoptosis, antioxidant effects, and neuroprotective activity in the treatment of spinal cord injuries [20–22]. Our investigations further reveal that Cur exerts a significant regulatory effect on microglial responses, fostering anti-inflammatory microglial polarization while inhibiting microglia-mediated pro-inflammatory reactions. Post-treatment with Cur has been shown to diminish brain damage induced by ischemic stroke and enhance functional outcomes [7,15]. This suggests that Cur holds promise as an antioxidant medication for scavenging ROS and modulating microglial polarization in the context of poststroke rehabilitation. These findings highlight the potential therapeutic role of Cur in mitigating the detrimental effects of stroke and improving overall recovery outcomes.

However, several constraints have hindered the clinical translation of Cur in poststroke rehabilitation. Firstly, Cur is a hydrophobic drug, necessitating the use of drug carriers to enhance its solubility in aqueous solutions. Secondly, owing to the gradual recovery of the blood−brain barrier (BBB) during the subacute phase, intravenous injection of the drug faces challenges in crossing the BBB to achieve sufficient concentration in the brain [23]. Although intracranial injection can directly deliver the drug into the stroke cavity, cerebrospinal fluid circulation may rapidly remove it from the brain [24,25]. Therefore, an ideal drug carrier should not only target the stroke cavity but also ensure sustained on-site drug release. An injectable hydrogel, administered in liquid form, capable of forming a hydrogel in situ and releasing the drug continuously on-site, aligns with this requirement [26]. Thirdly, employing smart release behaviors, such as stimuli-responsive release, can significantly enhance drug bioavailability and pharmaceutical efficacy. To optimize ROS scavenging, loading Cur into a ROS-sensitive release system could yield superior results. Consequently, an injectable hydrogel that is ROS-sensitive, directly delivered to the stroke cavity, and releases the drug in response to ROS cues emerges as the most suitable carrier for loading Cur in poststroke rehabilitation. These considerations address key challenges in Cur delivery, providing a foundation for enhanced therapeutic outcomes in stroke recovery.

In this study, hydroxypropyl-β-cyclodextrin (HP-β-CD) was employed to include Cur, forming a hydrophilic HP-β-CD/Cur inclusion complexes (Cur IC) [27–32]. The formation of hydrophilic Cur IC by the cyclodextrin chemistry solves one of main obstacles in the Cur delivery and could be loaded in the hydrogel carrier to be delivered targeting to the stroke cavity. Spontaneously, an injectable was generated through the Michael Addition of 4-arm polyethylene glycol acrylate (4-PEGA) and DL-dithiothreitol (DTT). The hydrogel, containing sulfur, exhibited ROS-sensitive degradation, providing a basis for ROS-sensitive release of the encapsulated drug. In another word, the hydrogel is able to eliminate extracellular ROS. Hence, the hydrogel not only serves as an inert carrier but also have pharmacological functions [33] to treat ROS accumulation after stroke. The hydrophilic Cur IC was then incorporated into the hydrogel precursor solution and directly injected into the stroke cavity, gelling in situ to produce the Cur IC loaded hydrogel (Cur gel). It is expected that Cur IC can be released in the peri-infarct zone from the hydrogel due to the ROS accumulation caused by the stroke to scavenge intracellular ROS by inhibiting the microglial to produce ROS, and simultaneously the ROS sensitive hydrogel can scavenge extracellular ROS. This double ROS-scavenging effect effectively regulates the anti-inflammatory polarization of the microglial so as to significantly enhance neuroplasticity to promote poststroke rehabilitation.

2. Experiments

2.1. Materials

Cur was purchased from Beijing Inoke Technology Co., Ltd., Beijing China, and hydroxypropyl-beta-cyclodextrin (HP-β-CD, > 99 %, Mw = 1431-1806 g/mol) was bought from Shanghai McLin Bio-chemical Technology Co., Ltd., Shanghai, China. 4-arm polyethylene glycol acrylate (4-PEGA, > 95 %, Mn = 10,000 g/mol) was bought from Beijing Key Technology Co., Ltd., Beijing, China, and DTT was bought from Hebei Bailingwei Superfine Material Co., Ltd., Hebei, China. The primary antibodies used in this study were listed in the supporting information.

2.2. Preparation and characterization of the Cur gel

2.2.1. Preparation of the Cur gel

73.6 mg of Cur (0.0002 mol) and 682 mg of HP-β-CD (0.0004 mol) were dissolved Cur in 24 mL anhydrous ethanol and HP-β-CD in 36 mL distilled water, respectively. The Cur solution was added to the HP-β-CD solution slowly and stirred for 1 h. The precipitate was removed by filtration and the ethanol was removed by rotation evaporation. The Cur IC was obtained by lyophilization. The Cur was dissolved in ethanol with different concentrations (2, 4, 8, 16, 20 and 30 μg/mL) and measured by UV spectrum. Subsequently, a standard curve (Fig. S3c) was obtained from the measured UV spectra. Then, the UV spectrum of Cur IC was mesasured in water and the content of Cur (3.7 wt%) in the IC was determined by using the standard curve.

44 mg of Cur IC and 330 mg 4-PEGA was dissolved in 1.5 mL of PBS buffer. 20 mg DTT was dissolved in 0.5 mL PBS. The two solutions were mixed and poured in a mold, then gelated at 37 °C to prepare the Cur gel.

IR measurement was conducted in FT-IR (Shimadzu IRTrace-100). UV measurement was performed on UV-Vis spectrophotometer (UV-1800). ^{1}H NMR spectra and 2D Nosey NMR were carried on 400M Liquid Nuclear Magnetic Resonance Spectrometer (Bruker AVANCE III 400 MHz). The detailed methods of characterizations are available in the supporting information.

2.2.2. Simulated ROS scavenging test

1 mg of 1, 1-diphenyl-2-pyridine hydrazine (DPPH) was dissolved in 20 mL of anhydrous ethanol to prepare DPPH solution. Add the appropriate amount of DPPH solution to each small glass bottle size 1 to 5. Bottle 1 was not treated, bottle 2 was added with ascorbic acid solution with equal concentration of 1 mg/mL, bottle 3 was added with blank gel, bottle 4 was added with Cur inclusion compound solution with equal concentration of 1 mg/mL, and bottle 5 was added with C gel. Observe the color change of the solution in the bottle.

2.3. In vitro cell experiments

2.3.1. In vitro regulation of microglia polarization

The biocompatibility of Cur IC against BV2 cells (mouse microglia cell line) with low (7.5 μM), medium (25 μM) and high (50 μM) concentrations were measured by CCK-8 assay. The biocompatibility of Cur gel against N2a cell was measured by live-dead cell assay.

BV2 cells were cultured in an OGD tank containing 95 % N_2 and 5 %

CO_2, using a sugar-free medium for 3 h. Subsequently, the medium was replaced with a sugar-containing medium, and the required substances were added in different experimental groups. After 24 h under oxygen and glucose conditions, BV2 cells were collected for analysis. The cells were then processed to obtain whole-cell lysates, and the expressions of CD16, CD206, IL-1β, and TGF-β, along with the phosphorylated forms of p65 (p-p65) and p65 in BV2 cells, were detected using Western Blot (WB). Furthermore, the expression of p47-*phox* and p67-*phox* in cell membrane and cytoplasm was detected by WB assay.

2.3.2. *In vitro enhancement of neuroplasticity by polarized BV2*

BV2 cells were divided into four groups (control, blank gel, Cur solution, and Cur gel) and cultured in the upper chamber of a transwell system for 12 h. Simultaneously, N2a cells were divided into two groups (N2a without OGD and N2a with OGD) and cultured in the lower plate of the transwell system. The four different groups of BV2 cells were placed on the transwell lower plate, each interacting with the two different N2a cell groups, resulting in the formation of eight complete transwell systems. Subsequently, the co-culture of BV2 cells with N2a cells was maintained for 24 h. Cell viability was assessed using the CCK-8 method. The expression of synaptophysin and PSD95 was determined through WB.

2.3.3. *In vitro ROS detection*

BV2 cells in different groups were collected and the intracellular ROS content was detected using Reactive Oxygen Species Assay Kit (S0033) and Amplex™ Red peroxide/peroxidase assay kit (A22188).

2.4. *In vivo experiments*

All *in vivo* studies were conducted following the approval of the Animal Experiment Ethics Committee of Beijing Rehabilitation Hospital, Capital Medical University. All animal care, housing, surgical, and anesthetic procedures were performed in accordance with EU Directive 2010/63/EU for animal experiments. The animals were housed in groups of five per cage at a standard temperature of 22 ± 1 °C, with free access to food and water. Male C57BL/6 J mice, aged 12 weeks and weighing 26.0 ± 1.5 g, were employed in the experiments.

The stroke of mice was induced by photothrombic (PT) method stroke accroding to our previous work [11,12]. On the 7th day post-stroke, 6.6 mg 4-PEGA was dissolved in 30 μL Cur IC's PBS buffer solution (29.3 mg/mL). Subsequently, the solution was mixed with 10 μL DTT PBS buffer solution (40 mg/mL) to get the precursor solution. Then, a 3 μL precursor solution of Cur gel was injected into the stroke cavity with liquid form and allowed to gel in situ. Mice were euthanized on the 21st day after the stroke. Initially, the mice were anesthetized with pentobarbital sodium and subsequently injected with 0.9 % normal saline followed by a 4 % paraformaldehyde (PFA) solution. The brain tissue was then removed and fixed in 4 % PFA solution. Microglial polarization *in vivo* was assessed through WB and Immunofluorescence (IF) staining. *In vivo* neuroplasticity was characterized using WB, IF staining, and Golgi staining (Servicebio, GP1152). *In vivo* content of reactive oxygen species (ROS) was determined through the DHE probe method.

The degradation of Cur gel in the mice was observed using the small animal fluorescence imaging system (IVIS®Lumina III, PerkinElmer, USA). Fluorescence imaging was performed at 7, 9, 14 and 21 days after stroke.

Ethological assessments, including the Rotarod and Balance Beam tests, were conducted on days 6, 8, 11, 14, and 21 after the stroke. In the Rotarod test, mice were trained on the Panlab Rotarod LE8505 for 3 days at 10 rpm prior to the formal experiment. During the official test, the Rotarod's speed was set to smoothly accelerate from 4 rpm to 40 rpm over 5 min, with the time taken for each mouse to drop off the shaft recorded. The test was repeated three times for each mouse. For the Balance Beam test, mice were trained to traverse the balance beam from one side three days before the formal experiment. The number of times the mouse's right hind paw fell from the balance beam was counted, and each mouse underwent the test three times.

2.5. *Statistics*

Statistical analysis of the experimental results was performed using GraphPad Prism software, and the results were expressed as mean ± standard deviation (SD). The unpaired parameter T-test was used to compare the two groups of data. Multiple comparisons of differences between groups were tested using One-way ANOVA. In all analyses, $p < 0.05$ was considered statistically significant, where $^{*}p < 0.05$, $^{**}p < 0.01$ and $^{***}p < 0.001$.

3. Results and discussion

3.1. *Preparation and characterization of Cur-cyclodextrin complex loaded hydrogel*

3.1.1. *Preparation and characterization of Cur IC*

As illustrated in Fig. 1a, the soluble Cur IC was prepared by incorporating Cur into the cavity of HP-β-CD. The molecular structure of Cur IC was simulated by DFT calculation. The results of DFT calculation in Fig. 1b show that the inclusion compound is formed by the molar ratio of 2:1 between HP-β-CD and Cur, and the benzene as well as the substituted methyl and hydroxyl moieties in the benzene are included by HP-β-CD. The formed Cur IC is further characterized by IR and NMR in Fig. 1c, Figs. S1 and S2. The NMR spectra in Fig. 1b shows the resonance peaks derived from both Cur and HP-β-CD occurs in the IC's NMR spectrum. The XRD spectra in Fig. 1d showed the Cur's crystalline structure disappears in the IC whereas it remains in the physical mixture.

3.1.2. *Preparation and characterization of Cur gel*

The successful preparation of the hydrogel was validated through the inverted vial experiment in Fig. 1f, while the SEM image in Fig. S5 showcases the porous structure of the hydrogel. The gelation time was determined to be 5 min at 37 °C and 8 min at 25 °C by inverted vial experiment. This gives enough time for the surgeons to deliver the hydrogel's liquid precursor solution to the stroke cavity and avoid the risk of gelation during the delivery. The mechanical properties of the hydrogel were measured by rheometer in Fig. S6, where the storage modulus is higher than the loss modulus indicating the successful gelation. *In vitro* degradation and release behaviors of the hydrogel are presented in Fig. 1g and h, respectively, demonstrating sustainable release of Cur IC for up to three weeks. Notably, the ROS environment significantly accelerates hydrogel degradation, leading to a faster release of Cur IC. Given that stroke-induced ROS accumulation in the cavity is a known occurrence, the intracranially delivered hydrogel can dynamically modulate the release of loaded Cur IC to influence microglia polarization based on the local ROS level. Cytocompatibility with BV2 microglial cells was assessed in Fig. 1i, revealing similar cell viabilities between Cur IC, Cur gel, and the control under low (7.5 μM) and intermediate (25 μM) Cur concentrations, with noticeable decrease observed under high (50 μM) Cur concentration. Consequently, the intermediate concentration was chosen for subsequent experiments due to its favorable cytocompatibility with microglia. Further investigation of cytocompatibility with N2a cells using a live-dead assay demonstrated comparable amounts of live cells in the Cur IC and Cur gel groups to the control in Fig. 1j and Fig. S7, affirming the hydrogel's good compatibility with neurons. Consequently, the well-tolerated cytocompatibility of the prepared hydrogel with both microglia and neurons positions it as a suitable carrier for delivering therapeutic drugs to the brain.

Fig. 1k exhibits the simulated ROS scavenging ability of the Cur gel. 1, 1-diphenyl-2-pyridine hydrazine (DPPH) was used to simulate the production of ROS in the test. The color change in Fig. 1k shows the addition of vitamin C as a reducing agent can thoroughly scavenge the ROS, whereas the blank gel and the Cur solution also exhibits a certain

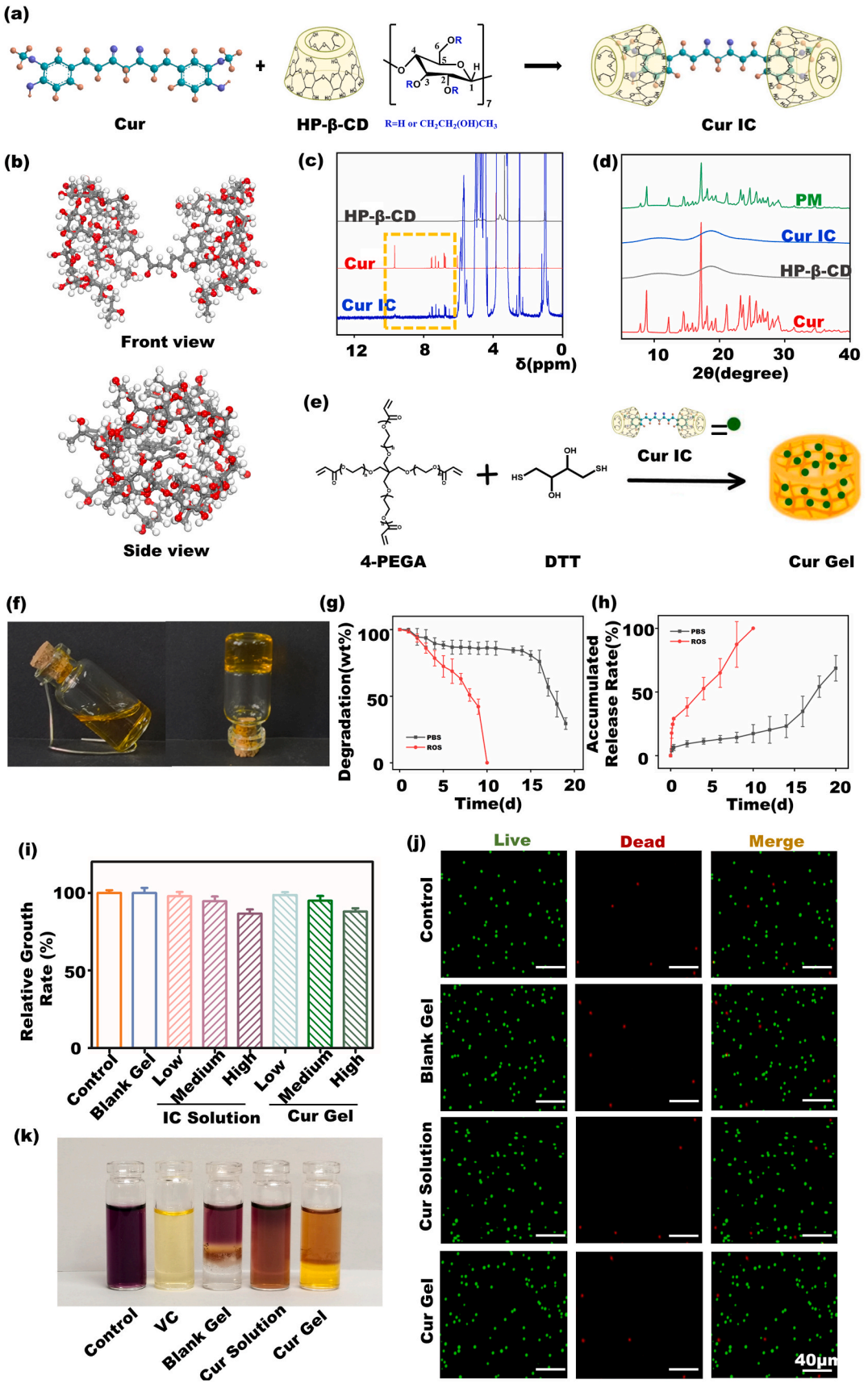

Fig. 1. Preparation and characterization of the Cur gel (a, reaction formula of Cur IC; b, optimized structure of Cur IC predicted by DFT calculation; c, ^{1}H NMR and d, XRD spectra; e, reaction formula of Cur gel; f, inverted vials; g, degradation and h, drug release of Cur gel *in vitro*; cytocompatibility of Cur gel against i, BV2 and j, N2a cells; k, simulated ROS scavenging test by Cur gel.

level of ROS scavenging ability. Interestingly, the Cur gel shows better ROS scavenging ability than the blank gel and the Cur solution. Thus, this test demonstrates both the blank gel and the Cur solution has the ability to eliminate ROS, and the Cur gel can combine their advantages and possess better ROS scavenging ability.

3.2. *In vitro ROS scavenging, microglia polarization and neuroplasticity regulated by Cur gel*

3.2.1. *In vitro ROS scavenging by Cur gel*

The *in vitro* ROS scavenging performance of the Cur gel is illustrated in Fig. 2a, b and 2c using the DCFH-DA fluorescent probe. OGD-treated microglia display heightened ROS accumulation, reflecting the pro-inflammatory polarization induced by OGD. Treatment with curcumin significantly reduces ROS expression in microglia, showcasing the excellent intracellular ROS-scavenging capability of the curcumin gel *in vitro*. Furthermore, the *in vitro* ROS scavenging was also conducted using Amplex™ Red assay in Fig. S8, which achieves similar results with the DCFH-DA probe.

3.2.2. *In vitro modulation of microglia polarization by Cur gel*

Fig. 2d-i investigates microglia polarization after OGD by WB. CD16 expression sharply increases after OGD, indicating pro-inflammatory microglial polarization induced by OGD treatment. Correspondingly, the pro-inflammatory factor IL-1β secreted by these microglia also increases after OGD. Treatment with both Cur IC and Cur gel significantly decreases the expression of CD16 and IL-1β, suggesting Cur's ability to suppress pro-inflammatory microglial polarization. Conversely, CD206 expression significantly decreases after OGD, accompanied by a corresponding decrease in the anti-inflammatory factor TGF-β. Treatment with both Cur IC and Cur gel significantly increases the expression of CD206 and TGF-β, indicating that Cur promotes microglial polarization toward the anti-inflammatory phenotype. Therefore, Fig. 2e-i demonstrate that Cur treatment effectively shifts microglial polarization from pro-inflammatory to anti-inflammatory phenotype after OGD.

3.2.3. *Anti-inflammatory microglia regulated by Cur gel to enhance neuroplasticity*

Fig. 2j schematically illustrates the transwell system used to assess the modulation of anti-inflammatory microglia on neuron neuroplasticity. In the upper chamber, microglia were cultured and polarized towards an anti-inflammatory phenotype by the Cur gel. Subsequently, the upper chamber with anti-inflammatory microglia was co-cultured with neurons in the transwell system. Fig. S9 depicts the viability of neurons after co-culture. The viability of neurons significantly decreases after OGD, indicating neuronal apoptosis. When OGD neurons are co-cultured with three OGD microglia, cell viability continues to decrease, aligning with the pathological consequences of ischemic stroke, where pro-inflammatory microglia exacerbate the local microenvironment, leading to further neuronal apoptosis. However, among the three co-culture groups, where OGD microglia were treated with a blank gel, Cur IC, and Cur gel, respectively, Cur gel treatment demonstrated the highest viability, Cur IC ranked in the middle, and the blank gel was the least effective. This primarily suggests that anti-inflammatory microglia can mitigate neuronal apoptosis and enhance neuroplasticity. The WB results in Fig. 2j-m exhibit a complete similar trend to the cell viability results.

3.3. *In vivo ROS scavenging and microglia polarization regulated by Cur gel*

3.3.1. *In vivo imaging of the Cur gel*

The schematic protocol of the animal test is depicted in Fig. 3a. After PT induction at day "t", the Cur gel was injected at day "t+7." In vivo imaging of the Cur gel and ethological tests were conducted at predetermined time intervals, and the mice were sacrificed at day "t+21″ for further WB and IF measurements.

The *in vivo* image of the Cur gel is presented in Fig. 3b. As Cur emits fluorescence signals, the implanted Cur gel was visualized using a small animal fluorescence imaging system in Fig. 3b. Immediately after implantation, a robust fluorescence signal was observed, indicating successful intracranial delivery of the gel. The signal intensity gradually weakened over time, suggesting the gradual degradation of the gel and sustained release of Cur *in vivo*. The signal was still detectable on the 21st day. This implies that the Cur gel can persist in the stroke cavity for an extended duration, facilitating sustained Cur release to modulate microglial polarization.

3.3.2. *In vivo ROS scavenging*

ROS levels in the infarct area of stroke mice were assessed through dihydroethidium (DHE) staining in Fig. 3c and d and S10. The sham group exhibited the lowest ROS expression, while the stroke group displayed the highest ROS expression, indicating severe oxidative stress post-stroke. Consistent with the *in vitro* tests, Cur treatment significantly reduced ROS levels in the infarct area. Additionally, the blank gel group demonstrated ROS levels between the stroke group and the two Cur-treated groups, indicating the pharmacological effect of the hydrogel in eliminating extracellular ROS *in vivo*. Notably, the Cur gel exhibited even lower ROS levels than the Cur IC group, underscoring its outstanding *in vivo* anti-oxidative ability.

3.3.3. *WB measurement for the in vivo modulation of microglia polarization by Cur gel*

Fig. 3e-g depict the modulation of microglial polarization by the Cur gel *in vivo.* Since microglia do not polarize in healthy mice, the sham group exhibits relatively low levels of both CD16 and CD206 expression. In contrast, stroke mice show the highest CD16 and the lowest CD206 expression, indicating microglial polarization toward a pro-inflammatory phenotype. However, both the Cur IC and Cur gel display significantly lower CD16 and higher CD206 expression than the stroke group, suggesting that Cur can regulate microglial polarization toward an anti-inflammatory phenotype *in vivo*. Furthermore, the performance of Cur IC in regulating the anti-inflammatory polarization of microglia is weaker than that of the Cur gel, as it exhibits noticeably higher CD16 and lower CD206 expression than the Cur gel.

3.3.4. *IF staining results for the in vivo modulation of microglia polarization by Cur gel*

Fig. 4 presents IF images of IBA-1/iNOS and IBA-1/CD206 co-staining to further investigate the *in vivo* polarization of microglia in the peri-infarct area in stroke mice. IBA-1 serves as a specific marker of activated microglia, where the colocalization of Iba-1$^+$iNOS$^+$ signifies proinflammatory microglia, while that of Iba-1$^+$CD206$^+$ corresponds to anti-inflammatory microglia. Given that most microglia remain at rest in healthy mice, Iba-1 expression is notably weak in the sham group. After stroke induction, Iba-1 expression becomes much stronger in other groups, indicating microglial activation due to PT ischemic stroke. Quantitative results of the colocalization of Iba-1$^+$iNOS$^+$ and Iba-1$^+$CD206$^+$ are presented in Fig. 4b and c. The stroke group exhibits the highest colocalization of Iba-1$^+$iNOS$^+$ and the lowest colocalization of Iba-1$^+$CD206$^+$, signifying proinflammatory microglial polarization resulting from ischemic stroke. In contrast, the Cur gel group displays the lowest colocalization of Iba-1$^+$iNOS$^+$ and the highest colocalization of Iba-1$^+$CD206$^+$, indicating that treatment with the Cur gel can alter microglial polarization from proinflammation to anti-inflammation. Thus, the co-staining of Iba-1/iNOS and Iba-1/CD206 reaffirms that the Cur gel can regulate microglial polarization toward an anti-inflammatory phenotype *in vivo*, corroborating the WB measurements in Section 3.3.2. Consistent with the WB results, the co-staining results also demonstrate that the Cur IC has weaker regulatory ability than the Cur gel in microglial polarization. Furthermore, the blank hydrogel exhibits lower colocalization of Iba-1$^+$iNOS$^+$ than the stroke group but

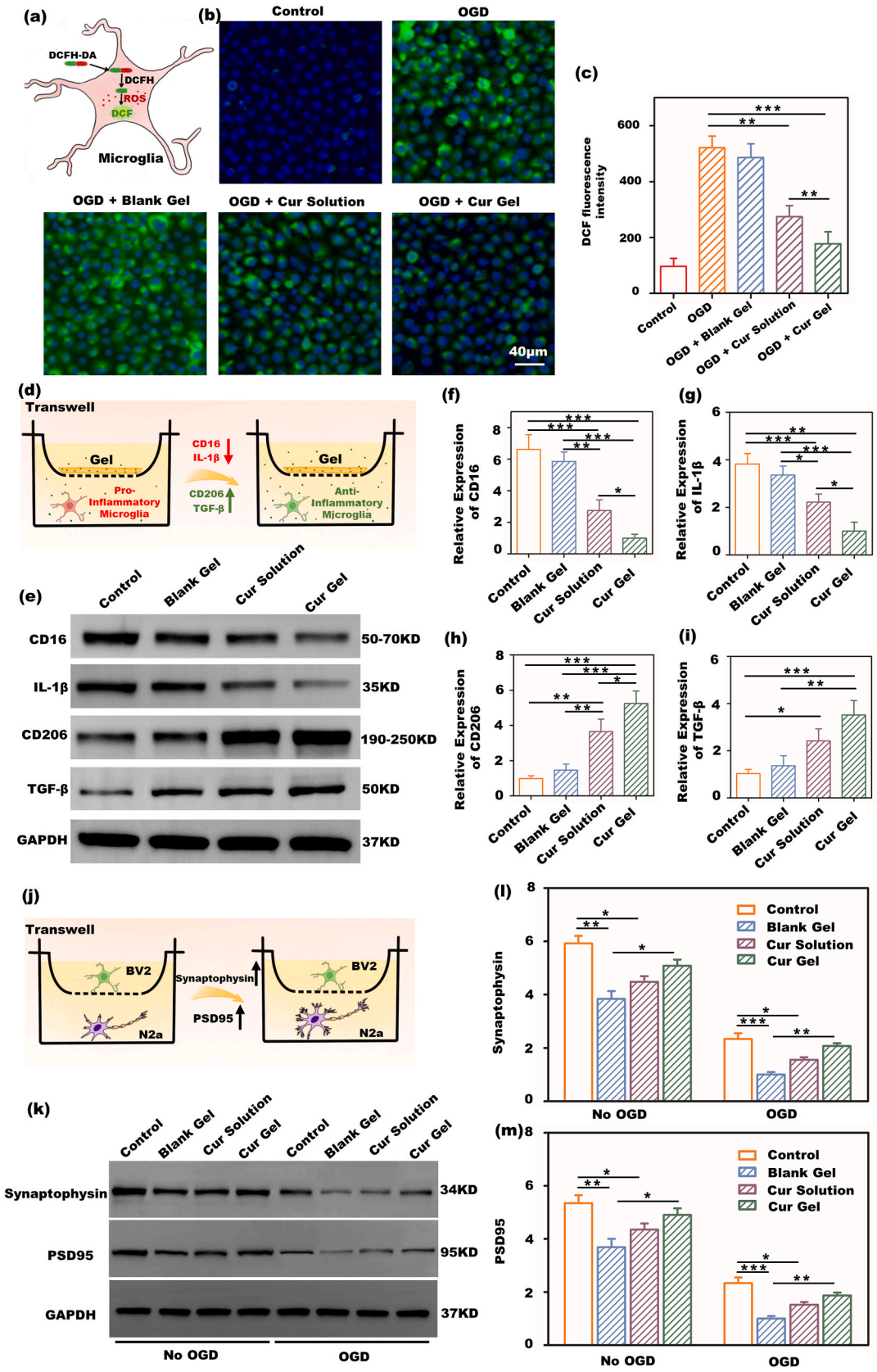

Fig. 2. *In vitro* tests of the Cur gel (a, schematic diagram of detecting *in vitro* ROS expression in BV2; b, IF images and c, quantitative results of ROS expression in BV2 cells; d, schematic diagram of BV2 polarization experiment; e, representative WB strips of BV2 polarization; quantitative results of f, CD16, g, IL-1β, h, CD206, i, TGF-β; j, schematic diagram of *in vitro* neuroplasticity experiment; k, representative WB strips and quantitative results of l, synaptophysin, m, PSD95) (*$p < 0.05$, **$p < 0.01$ and ***$p < 0.001$).

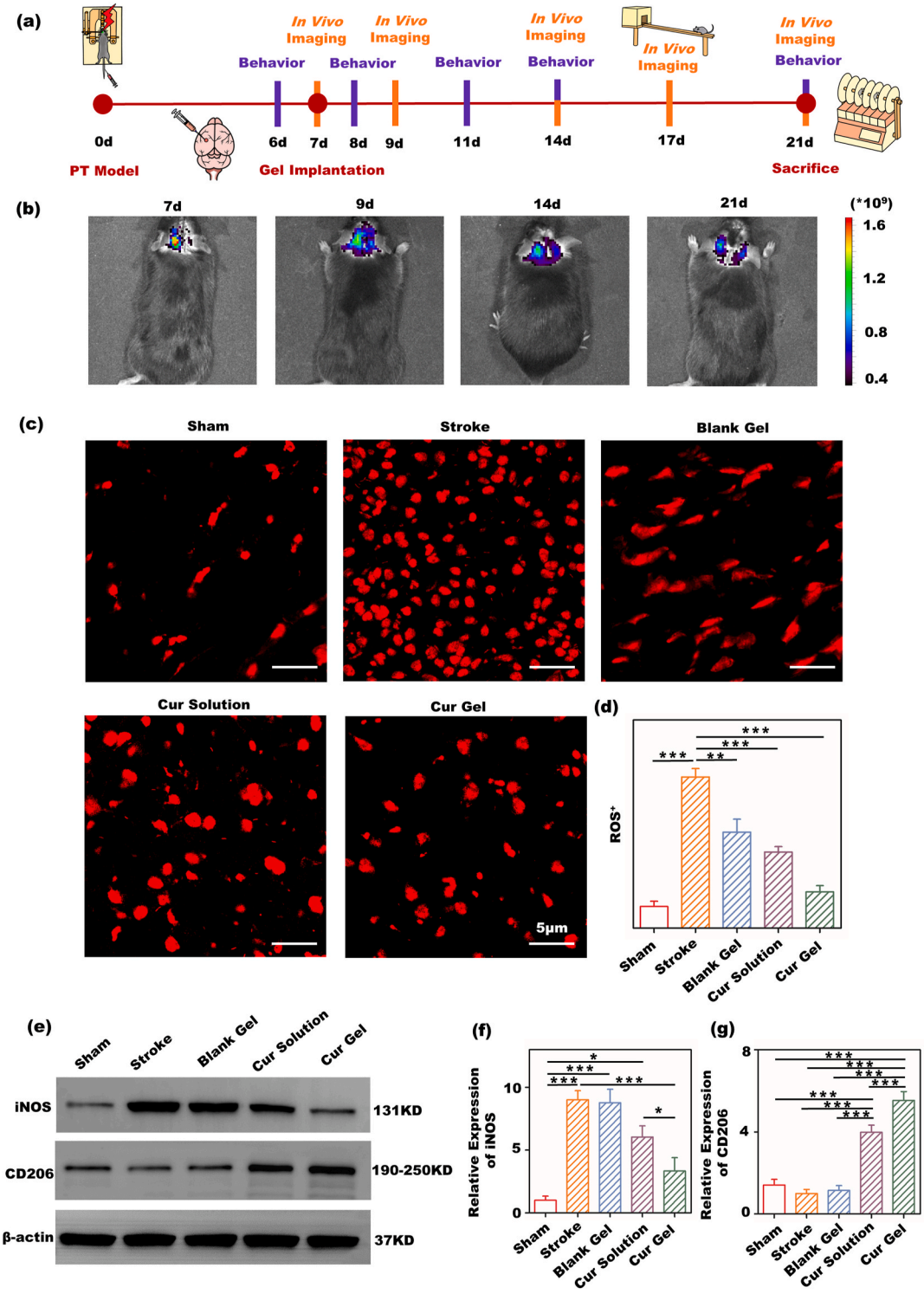

Fig. 3. *In vivo* experiment of the Cur gel (a, schematic diagram of *in vivo* experiment; b, fluorescence images of the implanted Cur gel under different implanted time; c, IF images and d, quantitative results of ROS expression *in vivo*; e, representative WB strips and quantitative results of f, synaptophysin, g, PSD95 *in vivo*). (*$p < 0.05$, **$p < 0.01$ and ***$p < 0.001$).

fails to achieve higher colocalization of Iba-1^{+}CD206^{+}, indicating that the blank gel may slightly lower pro-inflammatory microglial polarization but is unlikely to shift polarization from pro-inflammation to anti-inflammation.

3.4. Enhancement of in vivo neuroplasticity by Cur gel

3.4.1. In vivo synaptic plasticity by IF staining

Fig. 5 illustrate the synaptic plasticity of stroke mice evaluated through the co-staining of PSD95 and VGlut-1. PSD95 serves as a crucial scaffold protein in the postsynaptic membrane, while VGlut-1 is commonly employed as a presynaptic marker. The colocalization of

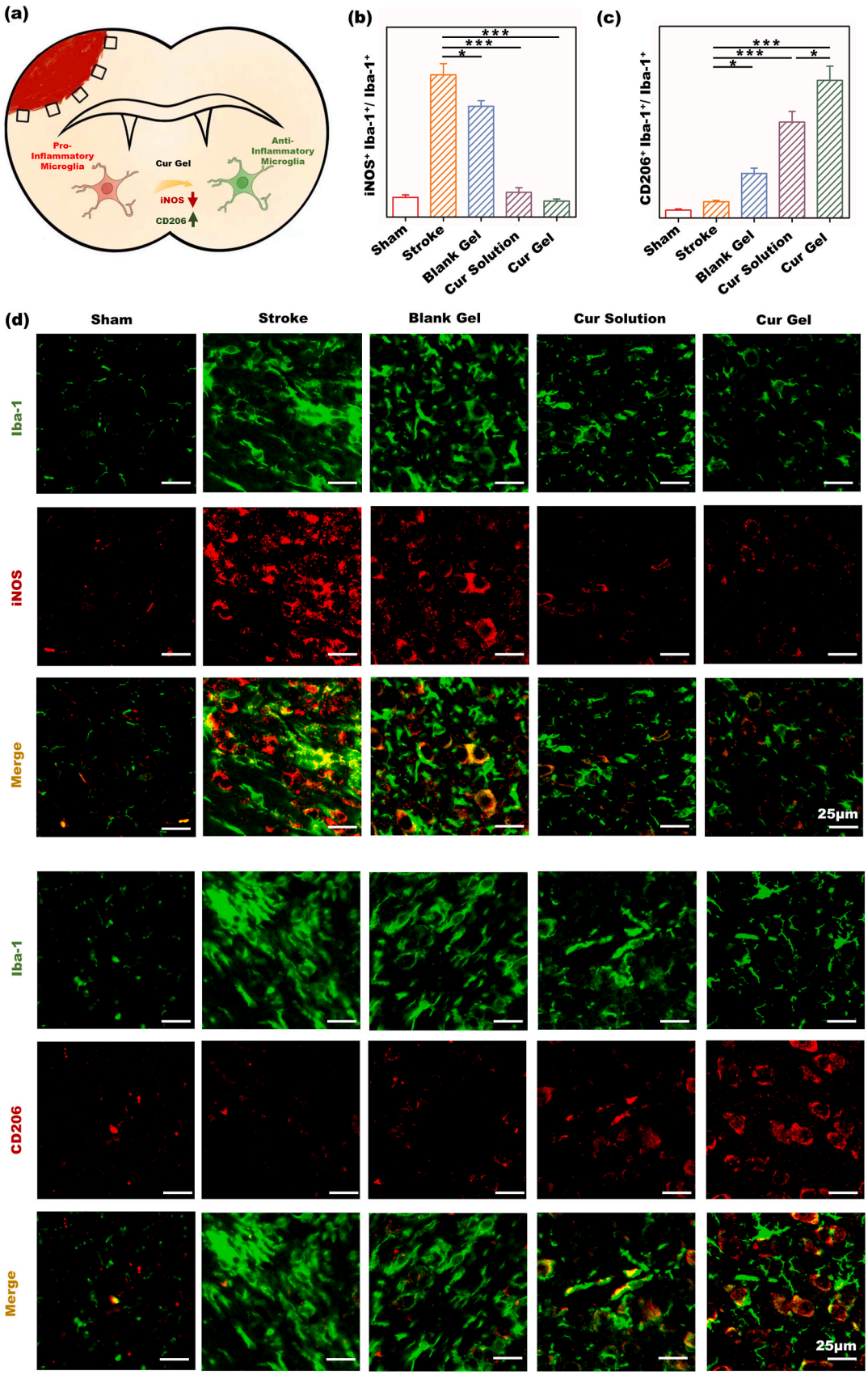

Fig. 4. *In vivo* microglial polarization modulated by the Cur gel. (a, schematic diagram of the areas for IF stain and quantitative calculation; quantitative results of b, Iba-1$^+$iNOS$^+$/Iba-1$^+$ and c, Iba-1$^+$CD206$^+$/Iba-1$^+$ percentage; IF images of Iba-1/iNOS and Iba-1/CD206 staining in the peri-infract zone of stroke mice) (*$p < 0.05$, **$p < 0.01$ and ***$p < 0.001$).

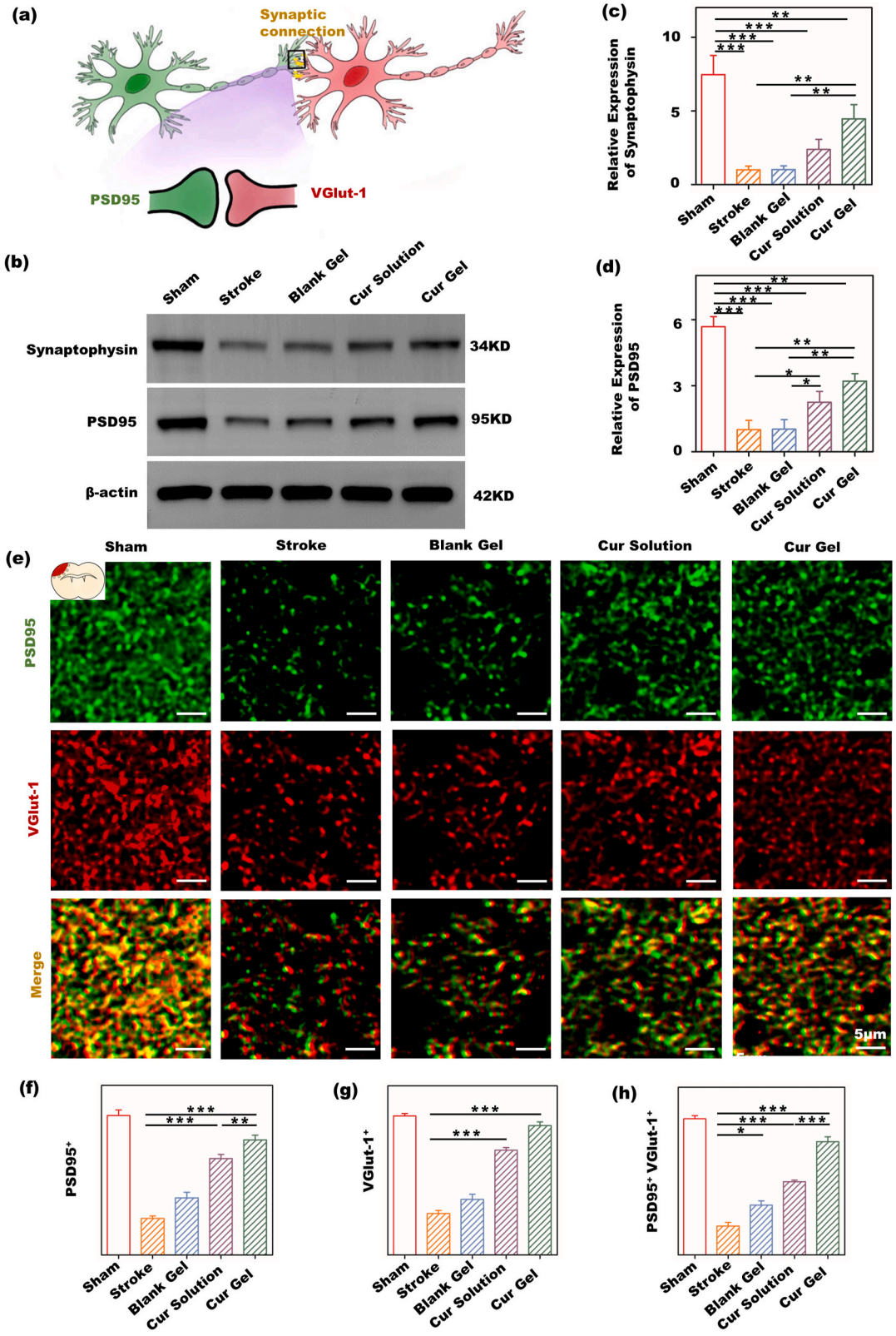

Fig. 5. *In vivo* synaptic plasticity enhanced by the Cur gel. (a, schematic diagram of synaptic connection characterized by PSD95 and VGlut-1 proteins; b, representative WB strips and quantitative results of c, synaptophysin, d, PSD95 *in vivo*; e, IF images of PSD95 and VGlut-1 staining in the peri-infract zone of stroke mice; quantitative results of f, $PSD95^{+}$, g, $VGlut\text{-}1^{+}$ and h, $PSD95^{+}VGlut\text{-}1^{+}$ area) (*$p < 0.05$, **$p < 0.01$ and ***$p < 0.001$).

$PSD95^{+}VGlut\text{-}1^{+}$ (depicted as orange dots in the merged images in Fig. 5e) signifies synaptic connections. Naturally, better synaptic connections indicate enhanced synaptic plasticity, which can further contribute to improved functional recovery. The expression of PSD95 and VGlut-1, as well as the colocalization of these two proteins, are depicted and calculated in Fig. 5f-h. A similar trend is observed for PSD95 and VGlut-1. The sham group exhibits the highest PSD95 and VGlut-1 expression, indicating perfect synaptic networks in healthy mice, while the stroke group displays the lowest PSD95 and VGlut-1 expression due to neuronal apoptosis caused by ischemic stroke. The treatment of the Cur gel can significantly increase PSD95 and VGlut-1 expression in the stroke mice, indicating the enhancement of synaptic plasticity *in vivo*. The Cur IC can also moderately increase PSD95 and VGlut-1 expression in the stroke mice. Unsurprisingly, the colocalization of $PSD95^{+}VGlut\text{-}1^{+}$ follows the same trend as PSD95 and VGlut-1 expression: the sham group has the best synaptic connections,

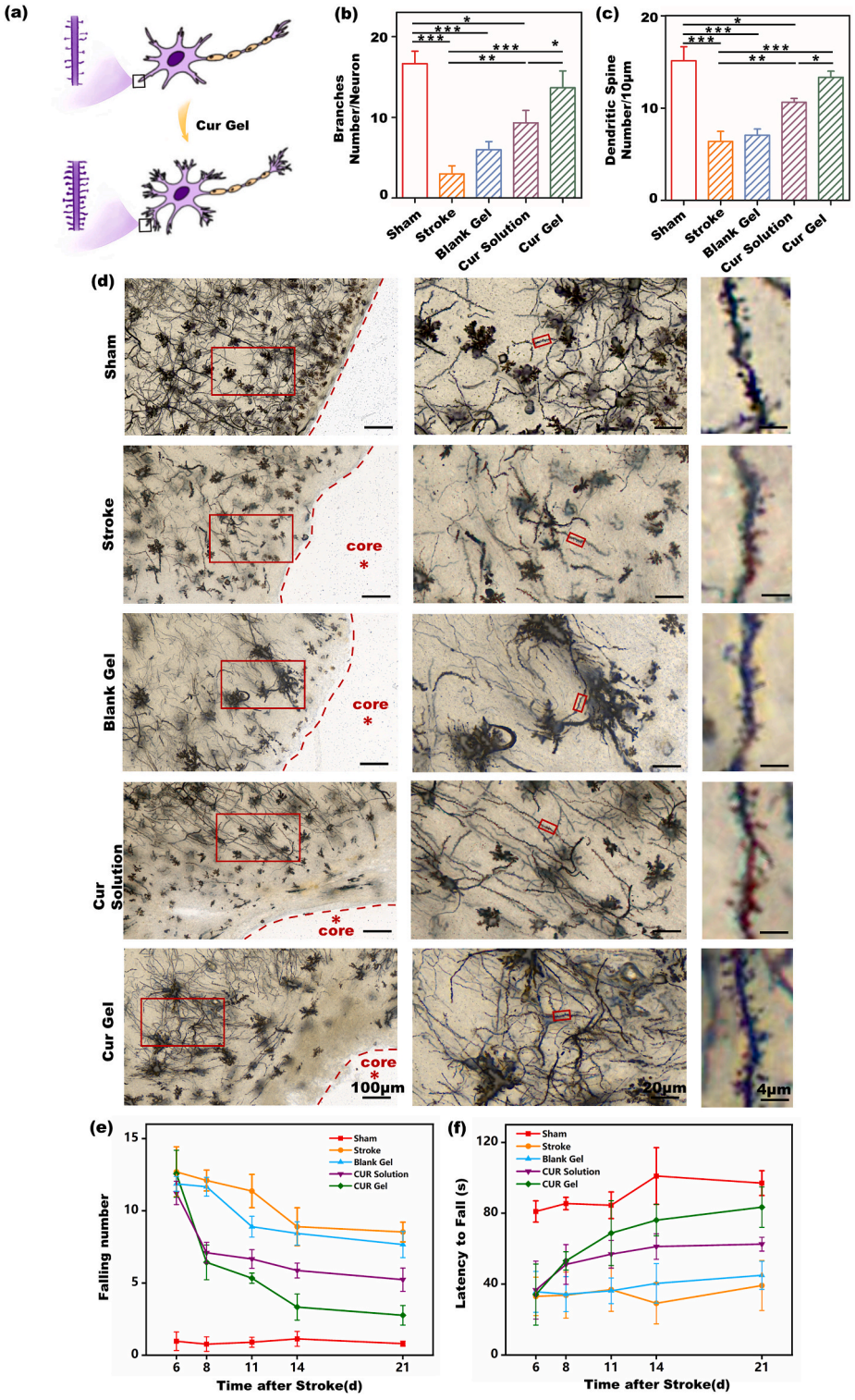

Fig. 6. *In vivo* dendritic plasticity enhanced by the Cur gel. (a, schematic diagram of dendritic spines; quantitative results of b, branch number and c, dendritic spine number *in vivo*; d, images of Golgi stains in the peri-infract zone of stroke mice; e, beam balance and f, rotarod results) (*$p < 0.05$, **$p < 0.01$ and ***$p < 0.001$).

followed by the Cur gel and Cur IC groups. Additionally, the WB results of synaptophysin and PSD-95 expression in Fig. 5b-d also demonstrate the recovery of synaptic plasticity by the Cur gel after PT stroke.

3.4.2. *In vivo dendritic plasticity by Golgi staining*

To investigate the effects of Cur gel treatment on dendritic spine structure after ischemic stroke, Golgi silver impregnation was performed to detect neuronal dendritic spines in the peri-infarct area, as shown in Fig. 6. PT stroke induces a significant reduction in the number of dendritic spines and branch numbers. Interestingly, Cur gel treatment markedly increased dendritic plasticity compared with that in the stroke group, indicating that Cur gel treatment can effectively enhance dendritic plasticity *in vivo*. Furthermore, Cur IC treatment also has positive influences on dendritic plasticity but is much weaker than the Cur gel. This finding is consistent with the result of synaptic plasticity.

3.4.3. *The ethological test*

Ethological tests, including the Balance Beam and Rotarod, were performed to assess the motor function recovery in stroke mice treated with Cur gel, as shown in Fig. 6e and f. In the Balance Beam test, the sham group consistently exhibits the lowest falling number throughout the treatment period, maintaining a stable low falling number. In contrast, the stroke markedly increases the falling number, with all groups except the sham group showing a similar baseline. Following gel administration, the Cur IC and Cur gel groups start to exhibit significant differences from the stroke and blank gel groups on the 8th day. By the 11th day, the Cur gel groups significantly outperform the Cur IC group, approaching the falling number of the sham group for the remainder of the treatment period. While the blank gel group has a slightly lower falling number than the stroke group, no statistical difference is observed. In the Rotarod test, the trend is opposite. The sham group consistently has the highest latency to fall throughout the treatment period, while the stroke significantly decreases this latency. Treatment with Cur gel gradually increases the latency, showing significant differences from the stroke group on the 11th day. By the 21st day, the latency to fall in the Cur gel group closely approaches that of the sham group, with no significant difference between them. The Cur IC also has positive effects to some extent. The blank gel group has a slightly higher latency to fall than the stroke group, but no statistical difference is observed.

3.5. *Modulation mechanism of Cur gel on the anti-inflammatory polarization of the microglia*

It has been reported that pro-inflammatory polarization can activate NADPH oxidase, leading to the production of ROS and pro-inflammatory cytokines in microglia [34]. The mechanism of dual ROS scavenging ability of the Cur gel is proposed in Fig. 7a. Furthermore, the translocation of cytosolic components such as p47-*phox* and p67-*phox* to the plasma membrane is crucial for the activation of NADPH oxidase [35–37]. Thus, the translocation of p47-*phox* and p67-*phox* was investigated by WB in Fig. 7b-f. The results show that p47-*phox* and p67-*phox* are primarily present in the cytoplasm in resting microglia. OGD treatment significantly increases the expression of p47-*phox* and p67-*phox* in the membrane while decreasing their expressions in the cytoplasm, indicating the translocation of p47-*phox* and p67-*phox*. Interestingly, the treatment of Cur gel significantly suppresses the translocation of p47-*phox* and p67-*phox*. Therefore, the *in vitro* results indicate that the Cur gel has a significant inhibitory effect on the translocation of p47-*phox* and p67-*phox*, which can scavenge intracellular ROS production by suppressing the activation of NADPH oxidase after stroke.

Given that the accumulation of ROS plays a crucial regulatory role in stroke-induced proinflammatory microglial polarization via the ROS-NF-κB signaling pathway [38,39], we further tested whether the Cur gel regulates anti-inflammatory microglial polarization by inhibiting the activation of the NF-κB signaling pathway in PT stroke models *in vitro* and *in vivo*. The protein expression of phosphorylated p65 (p-p65) (Fig. 7g-i) significantly increased in OGD microglia compared with those in resting microglia. However, the p-p65 expression as well as the ratios of p-p65/p65 significantly decrease after treatment with the Cur gel, implying the inhibition of NF-κB signaling by the Cur gel. The expression of NF-κB-related proteins was further investigated *in vivo* in Fig. 7j-l. Consistent with the *in vitro* results, Cur gel treatment dramatically inhibits the phosphorylation of p65 and reduces the ratios of p-p65/p65 in the peri-infarct area at 21 days after PT stroke. These findings indicate that the Cur gel significantly inhibits NF-κB activation in microglia after PT stroke by suppressing the translocation of p47-*phox* and p67-*phox*.

4. Discussion

As the cyclodextrins such as HP-β-CD can serve as hosts in the formation of ICs with lipophilic compounds, they have been successfully used as auxiliaries to solubilize drugs that are poorly soluble since the middle of the last century [27]. Besides IR and NMR results, the IC possesses the same UV spectrum (Fig. S3a) with Cur's UV spectra in ethanol (Fig. S3b) [40,41], and the 2D NOESY in Fig. S4 reveals the presence of the Overhauser effect between the phenolic hydrogen, the aromatic hydrogens of the Cur and H3, H5, H6 of the HP-β-CD, providing convincing evidence of the inclusion interaction between Cur and HP-β-CD. Therefore, the collective evidence from NMR, XRD and UV spectra confirms the successful preparation of the Cur IC. Having obtained the hydrophilic Cur IC through the inclusion of HP-β-CD, it can be efficiently loaded into the injectable hydrogel. As depicted in Fig. 1e, the injectable Cur gel is formed by 4-PEGA and DTT through Michael addition under physiological pH (7.4) at body temperature without the need for any catalyst [42–45], making it well-suited for intracranial delivery. Furthermore, the hydrogel's sulfur atoms are easily oxidized to sulfone by ROS species, resulting in rapid hydrolysis of the networks and conferring ROS-sensitive release behavior. This enables intelligent regulation of the release of Cur IC based on the ROS levels in the environment. On the other hand, as shown in Fig. 1k, the ROS responsive hydrolysis of the Cur gel can also consume ROS, which endows the gel with the ability to eliminate extracellular ROS. Some researchers reported to fabricate the hydrogel with the different acrylate/thiol feed ratios ranging from 0.8 to 1.8 [46]. In that case, some free DTT and tethered DTT may be present in the formed hydrogel when the feed amount of DTT is excessive. The free DTT and tethered DTT were found to possess satisfatory anti-oxidant ability. In this study, since we hope the ROS species can be used to break the hydrogel network to promote the release of the Cur IC, the molar equivalent acrylate/thiol feed ratio was adopted to avoid the production of the free DTT to consume the ROS species.

Fig. 2a-c clearly demonstrated the released Cur can eliminate intracellular ROS *in vitro*. Hence, the double ROS scavenging effects including extracellular and intracellular ROS scavenging were primarily shown in Figs. 1k and Fig. 2a–c, respectively. Zhou et al. co-loaded retinoic acid and Cur into bovine serum albumin for the treatment of spinal cord injury [47]. They highlighted that ROS scavenging from microglia could inhibit its polarization toward a pro-inflammatory phenotype, thereby promoting the secretion of anti-inflammatory cytokines *in vitro*. Therefore, it is speculated that the double ROS scavenging effects of the Cur gel may have the potential to further regulate microglia polarization toward an anti-inflammatory phenotype. Fig. 2d-i proved that the Cur gel treatment can significantly induce microglia to polarize toward an anti-inflammatory phenotype. Microglia, being typical macrophages in the brain, are widely reported in the literature to suggest that anti-inflammatory macrophages are beneficial for tissue repair and regeneration. Our previous works have also reported that anti-inflammatory microglia can secrete neurotrophic factors to promote neuroplasticity [7–16]. Thus, it is anticipated that the anti-inflammatory polarization of microglia modulated by the Cur gel can further enhance neuroplasticity *in vitro*. Fig. 2j-m as well as Fig. S8

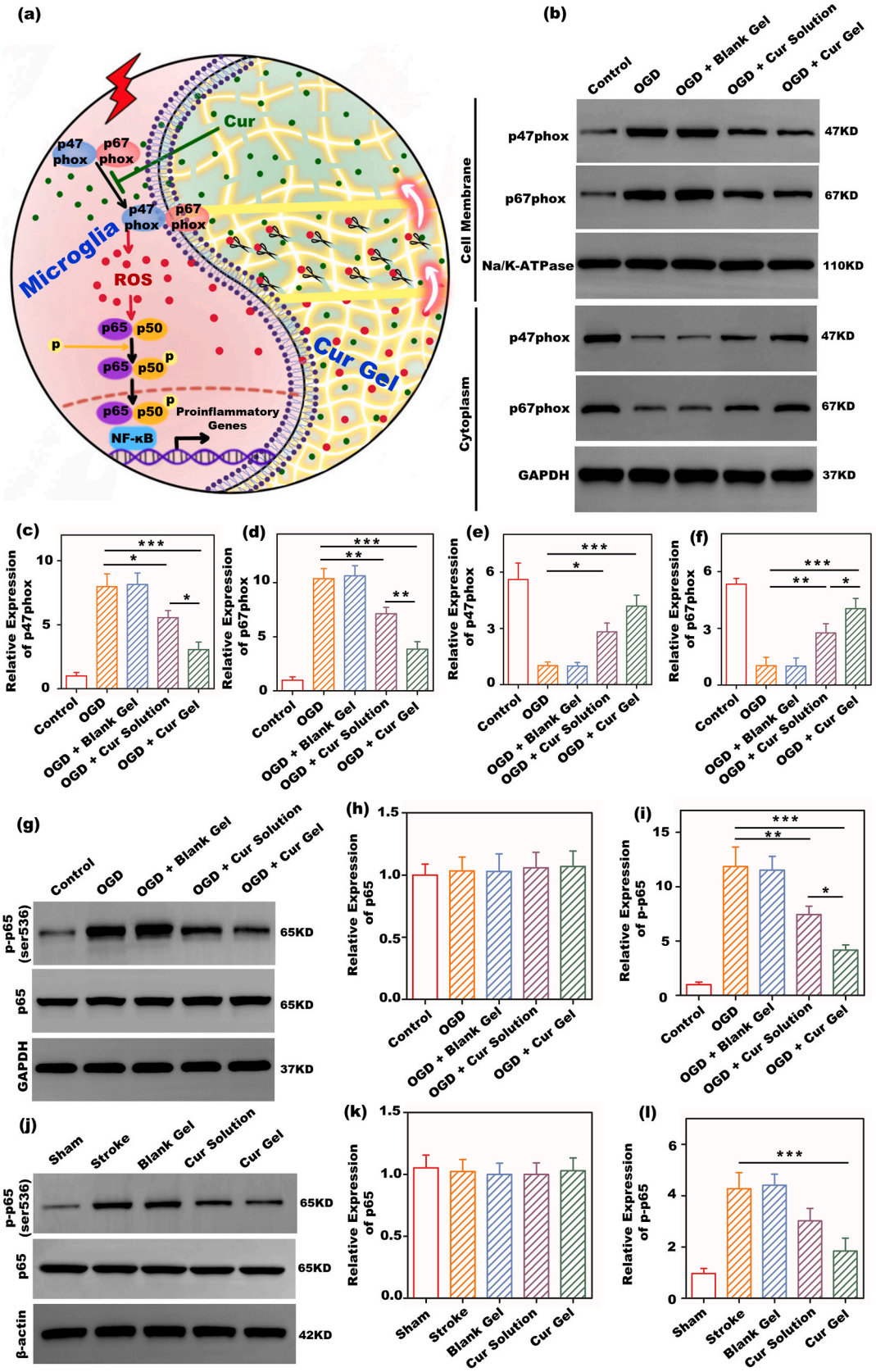

Fig. 7. The molecular mechanism of ROS scavenging by Cur gel via the translocation of p47-*phox* and p67-*phox*. (a, schematic diagram of double ROS scavenging effects of the Cur gel; b, representative WB stripes of p47-*phox* and p67-*phox* in the cell membrane and cytoplasm; quantitative results of c, p47-*phox*, d, p47-*phox* in the cell membrane and e, p47-*phox*, f, p47-*phox* in the cytoplasm; g, representative WB stripes and quantitative results of h, p65 and i, phosphorylated p65 (p-p65) *in vitro*; j, representative WB stripes and quantitative results of k, p65 and l, p-p65 *in vivo*) (*$p < 0.05$, **$p < 0.01$ and ***$p < 0.001$).

clearly showed the anti-inflammatory polarization of microglia regulated by the Cur gel can improve the neurons' viability and upgrade the expression of synaptophysin and PSD95. This reinforces the notion that anti-inflammatory microglia can mitigate neuronal apoptosis and enhance neuroplasticity, as synaptophysin and PSD95 are typical markers of synaptic plasticity.

Fig. 3c-d showed the Cur gel exhibits much better ROS scavenging performance than the Cur gel and other groups *in vivo*. On one hand, the Cur gel combines Cur's intracellular ROS elimination with the extracellular ROS elimination facilitated by the prepared gel, resulting in a double ROS-scavenging effect that endows the Cur gel with exceptional anti-oxidative capabilities. On the other hand, the more effective ROS elimination behavior of the Cur gel *in vivo* may stem from the hydrogel's sustained Cur release, ensuring a sufficiently high local drug concentration to continuously exert anti-oxidative effects in the stroke cavity. Wang and Zhang have highlighted that *in vivo* infiltration of certain nanozymes can initiate microglia polarization toward the anti-inflammatory phenotype by reducing ROS levels [49]. Similarly, Jiang et al. utilized a macrophage-disguised honeycomb manganese dioxide nanosphere loaded with fingolimod to reduce oxidative stress after ischemic stroke and promote the transition of pro-inflammatory microglia to the anti-inflammatory phenotype, ultimately reversing the pro-inflammatory microenvironment [48]. Thus, the outstanding ROS-scavenging ability of the Cur gel *in vivo* suggests its promising potential to regulate microglial polarization *in vivo*. Correspondingly, Fig. 3e-g and Fig. 4 demonstrated the Cur gel treatment can significantly promote microglia's anti-inflammatory polarization *in vivo*.

Microglial activation coincides with neuroplasticity after stroke, providing a fundamental basis for microglia-mediated inflammatory responses involved in entire neural network rewiring and brain repair. Microglial activation plays a crucial role in spontaneous recovery after stroke, contributing to the structural and functional reestablishment of neurovascular networks, neurogenesis, axonal remodeling, and blood vessel regeneration. Numerous studies [50–52], including ours [7–16], have demonstrated that modulating microglia toward anti-inflammatory polarization can promote neuroplasticity.

Synaptic plasticity plays a pivotal role in poststroke rehabilitation, directly impacting functional recovery after a stroke. It is widely acknowledged that poststroke rehabilitation, including motor function recovery, can be facilitated by enhancing neuroplasticity, such as synaptic plasticity [53–55]. Both IF and WB results in Fig. 5 support that the anti-inflammatory microglia regulated by the Cur gel can enhance synaptic plasticity the best among all the groups. Furthermore, dendritic spine densities, recognized as a cornerstone of functional restoration after stroke, constitute an independent indicator of poststroke recovery and are integral to neural structural and functional plasticity [56]. Dendritic plasticity plays a crucial role in the rebuilding of neural networks in the peri-infarct area. The increase in dendritic spine densities observed in surviving neurons adjacent to the infarct cavity contributes to reconstructing neural networks that take over the functions of lost neurons [57]. The Golgi staining and the semiquantitative results in Fig. 6a-d exhibited the Cur gel treatment can also significantly restore dendritic plasticity. Therefore, it can be concluded that Cur gel treatment after a stroke significantly enhances neuroplasticity in the peri-infarct zone.

The PT ischemic stroke typically leads to motor dysfunction [58], and several studies have demonstrated that poststroke functional outcomes are associated with increases in neuroplasticity [13,59]. As demonstrated in Figs. 5 and Fig. 6a–d, the Cur gel enhances both synaptic and dendritic plasticity, the motor function recovery was explored in Fig. 6e-f. The ethological results are in line with the *in vivo* microglial polarization and neuroplasticity findings. First, they suggest that Cur gel effectively restores the motor function of stroke mice, since it shows superior performance in modulating the anti-inflammatory polarization of microglia and enhancing neuroplasticity. Second, the Cur gel group exhibits better functional recovery than the Cur IC solution. As discussed earlier, this advantage arises from the hydrogel's pharmaceutically ROS-scavenging ability and sustainable Cur release behavior.

Additionally, the molecular mechanism of the Cur to scavenge the intracellular ROS and further regulate microglial polarization were investigated in Fig. 7. Both the *in vitro* and *in vivo* results indicate that the inhibitory effect of the Cur gel on proinflammatory microglial polarization is associated with Cur's ability to scavenge intracellular ROS by inhibiting the translocation of p47-*phox* and p67-*phox*, thereby suppressing the activation of the ROS-NF-κB signaling pathway after stroke.

In summary, the therapeutic mechanism of the Cur gel is illustrated in Scheme 1. In the context of PT ischemic stroke, proinflammatory microglia activated around the cavity release ROS. These released ROS oxidize sulfur in the hydrogel to sulfoxide, accelerating Cur IC release. Simultaneously, the released ROS are consumed by the hydrogel. The Cur IC released can be internalized by microglia, significantly inhibiting intracellular ROS production and promoting polarization towards an anti-inflammatory phenotype by inhibiting the translocation of p47-*phox* and p67-*phox*, thereby suppressing the activation of the ROS-NF-κB signaling pathway after stroke. Thus, the hydrogel exhibits a dual ROS-scavenging effect: Cur IC scavenges intracellular ROS, while the hydrogel eliminates extracellular ROS. Hence, the hydrogel not only serves as a carrier but also possesses pharmacological function to eliminate the extracellular ROS. Subsequently, the anti-inflammatory polarization of the microglial resulting from the double ROS scavenge effect can significantly enhance the neuroplasticity in the brain, and finally promote poststroke rehabilitation.

5. Conclusion

In this study, a Cur loaded hydrogel (Cur gel) with a double ROS-scavenging effect is synthesized. The sustainable release of the Cur IC is shown by *in vitro* drug release test. The intracellular ROS-scavenging capability of the Cur IC *in vitro* and *in vivo* were proven by the DCFH and DHE probe, respectively. The *in vitro* simulated ROS scavenging test shows the extracellular ROS elimination ability of the Cur gel. These fully demonstrates the double ROS-scavenging effect. Furthermore, the elimination of ROS effectively regulates microglial polarization towards an anti-inflammatory phenotype, which restores the expression of synaptophysin and PSD95 in OGD neurons, indicating an enhancement of *in vitro* neuroplasticity. Upon injection into the stroke cavity of mice, the Cur's modulation of microglial polarization and subsequent enhancement of neuroplasticity are further confirmed through IF staining, WB, and Golgi staining. Ethological measurements demonstrate the corresponding recovery of motor function. Both *in vitro* and *in vivo* findings collectively support the notion that the curcumin modulates anti-inflammatory microglia polarization by scavenging intracellular ROS through the inhibition of p47-*phox* and p67-*phox* translocation, thereby suppressing the activation of the ROS-NF-κB signaling pathway. Consequently, the injectable Cur gel emerges as a promising candidate for promoting poststroke rehabilitation in stroke mice by modulating microglial polarization to enhance neuroplasticity.

CRediT authorship contribution statement

Shulei Zhang: Writing – original draft, Investigation, Formal analysis. **Yuanyuan Ran:** Methodology, Funding acquisition, Formal analysis. **Yerasel Tuolhen:** Investigation. **Yufei Wang:** Investigation. **Guiqin Tian:** Project administration. **Jianing Xi:** Supervision. **Zengguo Feng:** Conceptualization. **Wei Su:** Supervision, Funding acquisition, Conceptualization. **Lin Ye:** Writing – review & editing, Supervision, Conceptualization. **Zongjian Liu:** Supervision, Funding acquisition, Conceptualization.

Declaration of competing interest

The authors declare that they have no known competing financial

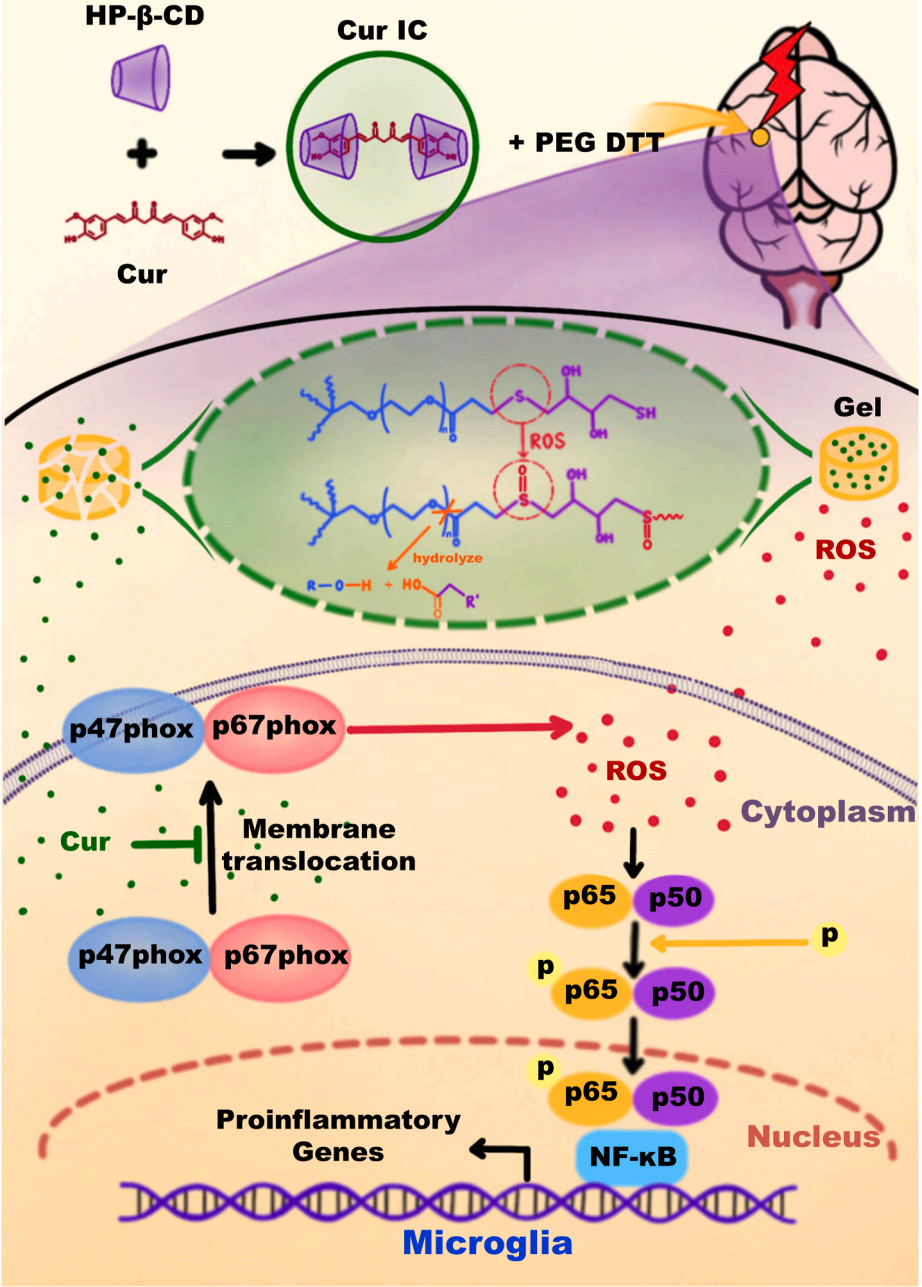

Scheme 1. Double ROS-scavenging effects of the Cur gel to promote poststroke rehabilitation.

interests or personal relationships that could have appeared to influence the work reported in this paper.

Data availability

Data will be made available on request.

Acknowledgments

This work is financially supported by Beijing Municipal Natural Science Foundation (7222102), National Natural Science Foundation of China (82271325, 82272616, 82102655).

Appendix A. Supplementary data

Supplementary data to this article can be found online at https://doi.org/10.1016/j.mtbio.2024.101177.

References

[1] V.L. Feigin, M. Brainin, B. Norrving, S. Martins, R.L. Sacco, W. Hacke, M. Fisher, J. Pandian, P. Lindsay, World stroke organization (WSO): global stroke fact sheet 2022, Int. J. Stroke 17 (1) (2022) 18–29.
[2] M. Katan, A. Luft, Global burden of stroke, Semin. Neurol. 38 (2) (2018) 208–211.
[3] G.L. Chimatiro, A.J. Rhoda, Scoping review of acute stroke care management and rehabilitation in low and middle-income countries, BMC Health Serv. Res. 19 (1) (2019) 1–15.
[4] L. Yang, B. Han, Z. Zhang, S. Wang, Y. Bai, Y. Zhang, Y. Tang, L. Du, L. Xu, F. Wu, L. Zuo, X. Chen, Y. Lin, K. Liu, Q. Ye, B. Chen, B. Li, T. Tang, Y. Wang, L. Shen, G. Wang, M. Ju, M. Yuan, W. Jiang, J.H. Zhang, G. Hu, J. Wang, H. Yao, Extracellular vesicle–mediated delivery of circular RNA SCMH1 promotes functional recovery in rodent and nonhuman primate ischemic stroke models, Circulation 142 (6) (2020) 556–574.
[5] S.E. Nadeau, X. Lu, B. Dobkin, S.S. Wu, Y.E. Dai, P.W. Duncan, A prospective test of the late effects of potentially antineuroplastic drugs in a stroke rehabilitation study, Int. J. Stroke 9 (4) (2012) 449–456.

[6] S. Hacene, A. Le Friec, F. Desmoulin, L. Robert, N. Colitti, J. Fitremann, I. Loubinoux, C. Cirillo, Present and future avenues of cell-based therapy for brain injury: the enteric nervous system as a potential cell source, Brain Pathol. 32 (5) (2022) e13105.
[7] Z. Liu, Y. Ran, S. Huang, S. Wen, W. Zhang, X. Liu, Z. Ji, X. Geng, X. Ji, H. Du, R. K. Leak, X. Hu, Curcumin protects against ischemic stroke by titrating microglia/macrophage polarization, Front. Aging Neurosci. 9 (2017) 233.
[8] Y. Ran, L. Ye, Z. Ding, F. Gao, S. Yang, B. Fang, Z. Liu, J. Xi, Melatonin protects against ischemic brain injury by modulating PI3K/AKT signaling pathway via suppression of PTEN activity, ASN Neuro 13 (2021) 17590914211022888.
[9] S. Qie, Y. Ran, X. Lu, W. Su, W. Li, J. Xi, W. Gong, Z. Liu, Candesartan modulates microglia activation and polarization via NF-κB signaling pathway, Int. J. Immunopathol. Pharmacol. 34 (2020) 2058738420974900.
[10] Y. Ran, S. Qie, F. Gao, Z. Ding, S. Yang, G. Tian, Z. Liu, J. Xi, Baicalein ameliorates ischemic brain damage through suppressing proinflammatory microglia polarization via inhibiting the TLR4/NF-κB and STAT1 pathway, Brain Res. 1770 (2021) 147626.
[11] Z. Liu, S. Zhang, Y. Ran, H. Geng, F. Gao, G. Tian, Z. Feng, J. Xi, L. Ye, W. Su, Nanoarchitectonics of tannic acid based injectable hydrogel regulate the microglial phenotype to enhance neuroplasticity for poststroke rehabilitation, Biomater. Res. 27 (1) (2023) 108.
[12] X. Ma, F. Gao, W. Su, Y. Ran, T. Bilalijiang, Y. Tuolhen, G. Tian, L. Ye, Z. Feng, J. Xi, Z. Liu, Multifunctional injectable hydrogel promotes functional recovery after stroke by modulating microglial polarization, angiogenesis and neuroplasticity, Chem. Eng. J. 464 (2023) 142520.
[13] F. Yu, T. Huang, Y. Ran, D. Li, L. Ye, G. Tian, J. Xi, Z. Liu, New insights into the roles of microglial regulation in brain plasticity-dependent stroke recovery, Front. Cell. Neurosci. 15 (2021) 727899.
[14] Z. Liu, D.M. Hermann, E. Dzyubenko, G. Cao, X. Cao, Editorial: modulating microglia to enhance neuroplasticity for restoring brain function after stroke, Front. Cell. Neurosci. 17 (2023) 1232437.
[15] Y. Ran, W. Su, F. Gao, Z. Ding, S. Yang, L. Ye, X. Chen, G. Tian, J. Xi, Z. Liu, W.-J. Tu, Curcumin ameliorates white matter injury after ischemic stroke by inhibiting microglia/macrophage pyroptosis through NF-κB suppression and NLRP3 inflammasome inhibition, Oxid. Med. Cell. Longev. 2021 (2021) 1–25.
[16] C. Qiao, Z. Liu, S. Qie, The implications of microglial regulation in neuroplasticity-dependent stroke recovery, Biomolecules 13 (3) (2023) 571.
[17] D. Yoo, A.W. Magsam, A.M. Kelly, P.S. Stayton, F.M. Kievit, A.J. Convertine, Core-cross-linked nanoparticles reduce neuroinflammation and improve outcome in a mouse model of traumatic brain injury, ACS Nano 11 (9) (2017) 8600–8611.
[18] F. Qian, Y. Han, Z. Han, D. Zhang, L. Zhang, G. Zhao, S. Li, G. Jin, R. Yu, H. Liu, In Situ implantable, post-trauma microenvironment-responsive, ROS Depletion Hydrogels for the treatment of Traumatic brain injury, Biomaterials 270 (2021) 120675.
[19] W. He, Z. Zhang, X. Sha, Nanoparticles-mediated emerging approaches for effective treatment of ischemic stroke, Biomaterials 277 (2021) 121111.
[20] R. Requejo-Aguilar, A. Alastrue-Agudo, M. Cases-Villar, E. Lopez-Mocholi, R. England, M.J. Vicent, V. Moreno-Manzano, Combined polymer-curcumin conjugate and ependymal progenitor/stem cell treatment enhances spinal cord injury functional recovery, Biomaterials 113 (2017) 18–30.
[21] N. Rahiman, Y.V. Markina, P. Kesharwani, T.P. Johnston, A. Sahebkar, Curcumin-based nanotechnology approaches and therapeutics in restoration of autoimmune diseases, J. Contr. Release 348 (2022) 264–286.
[22] R. Narayanamurthy, J.L.J. Yang, J.Y. Yager, L.D. Unsworth, Drug delivery platforms for neonatal brain injury, J. Contr. Release 330 (2021) 765–787.
[23] S. Bernardo-Castro, J.A. Sousa, E. Martins, H. Donato, C. Nunes, O.C. d'Almeida, M. Castelo-Branco, A. Abrunhosa, L. Ferreira, J. Sargento-Freitas, The evolution of blood–brain barrier permeability changes after stroke and its implications on clinical outcome: a systematic review and meta-analysis, Int. J. Stroke 18 (7) (2023) 783–794.
[24] J. Wang, X. Li, Y. Song, Q. Su, X. Xiaohalati, W. Yang, L. Xu, B. Cai, G. Wang, Z. Wang, L. Wang, Injectable silk sericin scaffolds with programmable shape-memory property and neuro-differentiation-promoting activity for individualized brain repair of severe ischemic stroke, Bioact. Mater. 6 (7) (2021) 1988–1999.
[25] L.R. Nih, P. Moshayedi, I.L. Llorente, A.R. Berg, J. Cinkornpumin, W.E. Lowry, T. Segura, S.T. Carmichael, Engineered HA hydrogel for stem cell transplantation in the brain: biocompatibility data using a design of experiment approach, Data Brief 10 (2017) 202–209.
[26] X. Ma, M. Wang, Y. Ran, Y. Wu, J. Wang, F. Gao, Z. Liu, J. Xi, L. Ye, Z. Feng, Design and fabrication of polymeric hydrogel carrier for nerve repair, Polymers 14 (8) (2022) 1549.
[27] Z. Liu, L. Ye, J. Xi, J. Wang, Z.G. Feng, Cyclodextrin polymers: structure, synthesis, and use as drug carriers, Prog. Polym. Sci. 118 (2021) 101418.
[28] P.R.K. Mohan, G. Sreelakshmi, C.V. Muraleedharan, R. Joseph, Water soluble complexes of curcumin with cyclodextrins: characterization by FT-Raman spectroscopy, Vib. Spectrosc. 62 (2012) 77–84.
[29] Z. Ma, N. Wang, H. He, X. Tang, Pharmaceutical strategies of improving oral systemic bioavailability of curcumin for clinical application, J. Contr. Release 316 (2019) 359–380.
[30] T.A. Hagbani, S. Nazzal, Curcumin complexation with cyclodextrins by the autoclave process: method development and characterization of complex formation, Int. J. Pharm. 520 (1–2) (2017) 173–180.
[31] A. Faridi Esfanjani, S.M. Jafari, Biopolymer nano-particles and natural nano-carriers for nano-encapsulation of phenolic compounds, Colloids Surf. B Biointerfaces 146 (2016) 532–543.
[32] A. Gupta, S.M. Briffa, S. Swingler, H. Gibson, V. Kannappan, G. Adamus, M. Kowalczuk, C. Martin, I. Radecka, Synthesis of silver nanoparticles using curcumin-cyclodextrins loaded into bacterial cellulose-based hydrogels for wound dressing applications, Biomacromolecules 21 (5) (2020) 1802–1811.
[33] F. Fang, S. Wang, Y. Song, M. Sun, W. Chen, D. Zhao, J. Zhang, Continuous spatiotemporal therapy of A full-API nanodrug via multi-step tandem endogenous biosynthesis, Nat. Commun. 14 (1) (2023) 1660.
[34] D.K. Dang, E.J. Shin, Y. Nam, S. Ryoo, J.H. Jeong, C.G. Jang, T. Nabeshima, J. S. Hong, H.C. Kim, Apocynin prevents mitochondrial burdens, microglial activation, and pro-apoptosis induced by a toxic dose of methamphetamine in the striatum of mice via inhibition of p47phox activation by ERK, J. Neuroinflammation 13 (1) (2016) 1–22.
[35] S. Shimohama, H. Tanino, N. Kawakami, N. Okamura, H. Kodama, T. Yamaguchi, T. Hayakawa, A. Nunomura, S. Chiba, G. Perry, M.A. Smith, S. Fujimoto, Activation of NADPH oxidase in alzheimer's disease brains, Biochem. Biophys. Res. Commun. 273 (1) (2000) 5–9.
[36] S. Wang, C.H. Chu, M. Guo, L. Jiang, H. Nie, W. Zhang, B. Wilson, L. Yang, T. Stewart, J.-S. Hong, J. Zhang, Identification of a specific α-synuclein peptide (α-Syn 29-40) capable of eliciting microglial superoxide production to damage dopaminergic neurons, J. Neuroinflammation 13 (1) (2016) 1–19.
[37] Y. Che, L. Hou, F. Sun, C. Zhang, X. Liu, F. Piao, D. Zhang, H. Li, Q. Wang, Taurine protects dopaminergic neurons in a mouse Parkinson's disease model through inhibition of microglial M1 polarization, Cell Death Dis. 9 (4) (2018) 435.
[38] J.C. Huang, Z.P. Yue, H.F. Yu, Z.Q. Yang, Y.S. Wang, B. Guo, TAZ ameliorates the microglia-mediated inflammatory response via the Nrf2-ROS-NF-κB pathway, Mol. Ther. Nucleic Acids 28 (2022) 435–449.
[39] J. Park, J.S. Min, B. Kim, U.B. Chae, J.W. Yun, M.S. Choi, I.K. Kong, K.T. Chang, D. S. Lee, Mitochondrial ROS govern the LPS-induced pro-inflammatory response in microglia cells by regulating MAPK and NF-κB pathways, Neurosci. Lett. 584 (2015) 191–196.
[40] S. Mondal, S. Ghosh, S.P. Moulik, Stability of curcumin in different solvent and solution media: UV-visible and steady-state fluorescence spectral study, J. Photochem. Photobiol. B Biol. 158 (2016) 212–218.
[41] A. Dutta, B. Boruah, A.K. Manna, B. Gohain, P.M. Saikia, R.K. Dutta, Stabilization of diketo tautomer of curcumin by premicellar anionic surfactants: UV–Visible, fluorescence, tensiometric and TD-DFT evidences, Spectrochim. Acta Mol. Biomol. Spectrosc. 104 (2013) 150–157.
[42] Y. Xiao, H. Zhao, X. Ma, Z. Gu, X. Wu, L. Zhao, L. Ye, Z. Feng, Hydrogel dressing containing basic fibroblast growth factor accelerating chronic wound healing in aged mouse model, Molecules 27 (19) (2022) 6618.
[43] X. Geng, Z.Q. Xu, C.Z. Tu, J. Peng, X. Jin, L. Ye, A.Y. Zhang, Y.Q. Gu, Z.G. Feng, Hydrogel complex electrospun scaffolds and their multiple functions in in situ vascular tissue engineering, ACS Appl. Bio Mater. 4 (3) (2021) 2373–2384.
[44] C. Tu, Y. Zhang, Y. Xiao, Y. Xing, Y. Jiao, X. Geng, A. Zhang, L. Ye, Y. Gu, Z. Feng, Hydrogel-complexed small-diameter vascular graft loaded with tissue-specific vascular extracellular matrix components used for tissue engineering, Biomater. Adv. 142 (2022) 213138.
[45] J. Peng, H. Zhao, C. Tu, Z. Xu, L. Ye, L. Zhao, Z. Gu, D. Zhao, J. Zhang, Z. Feng, In situ hydrogel dressing loaded with heparin and basic fibroblast growth factor for accelerating wound healing in rat, Mater. Sci. Eng. C 116 (2020) 111169.
[46] Y. Liu, R. Guo, T.L. Wu, Y. Lyu, M. Xiao, B.B. He, J.W. Fan, J.H. Yang, W.G. Liu, One zwitterionic injectable hydrogel with ion conductivity enables efficient restoration of cardiac function after myocardial infarction, Chem. Eng. J. 418 (2021) 129352.
[47] X. Gao, Z. Han, C. Huang, H. Lei, G. Li, L. Chen, D. Feng, Z. Zhou, Q. Shi, L. Cheng, X. Zhou, An anti-inflammatory and neuroprotective biomimetic nanoplatform for repairing spinal cord injury, Bioact. Mater. 18 (2022) 569–582.
[48] L. Feng, C. Dou, Y. Xia, B. Li, M. Zhao, P. Yu, Y. Zheng, A.M. El-Toni, N.F. Atta, A. Galal, Y. Cheng, X. Cai, Y. Wang, F. Zhang, Neutrophil-like cell-membrane-coated nanozyme therapy for ischemic brain damage and long-term neurological functional recovery, ACS Nano 15 (2) (2021) 2263–2280.
[49] C. Li, Z. Zhao, Y. Luo, T. Ning, P. Liu, Q. Chen, Y. Chu, Q. Guo, Y. Zhang, W. Zhou, H. Chen, Z. Zhou, Y. Wang, B. Su, H. You, T. Zhang, X. Li, H. Song, C. Li, T. Sun, C. Jiang, Macrophage-disguised manganese dioxide nanoparticles for neuroprotection by reducing oxidative stress and modulating inflammatory microenvironment in acute ischemic stroke, Adv. Sci. 8 (20) (2021) 2101526.
[50] Y.K. Yue, B. Mo, J. Zhao, Y.J. Yu, L. Liu, C.L. Yue, W. Liu, Neuroprotective effect of curcumin against oxidative damage in BV-2 microglia and high intraocular pressure animal model, J. Ocul. Pharmacol. Therapeut. 30 (8) (2014) 657–664.
[51] C. Duan, H. Wang, D. Jiao, Y. Geng, Q. Wu, H. Yan, C. Li, Curcumin restrains oxidative stress of after intracerebral hemorrhage in rat by activating the Nrf2/HO-1 pathway, Front. Pharmacol. 13 (2022) 889266.
[52] Y. Li, J. Huang, J. Wang, S. Xia, H. Ran, L. Gao, C. Feng, L. Gui, Z. Zhou, J. Yuan, Human umbilical cord-derived mesenchymal stem cell transplantation supplemented with curcumin improves the outcomes of ischemic stroke via AKT/GSK-3β/β-TrCP/Nrf2 axis, J. Neuroinflammation 20 (1) (2023) 49.
[53] G.M. Petzinger, B.E. Fisher, S. McEwen, J.A. Beeler, J.P. Walsh, M.W. Jakowec, Exercise-enhanced neuroplasticity targeting motor and cognitive circuitry in Parkinson's disease, Lancet Neurol. 12 (7) (2013) 716–726.
[54] M. Hong, M. Kim, T.W. Kim, S.S. Park, M.K. Kim, Y.H. Park, Y.H. Sung, M.-S. Shin, Treadmill exercise improves motor function and short-term memory by enhancing synaptic plasticity and neurogenesis in photothrombotic stroke mice, International Neurourology Journal 24 (Suppl 1) (2020) S28–S38.
[55] G. Di Pino, G. Pellegrino, G. Assenza, F. Capone, F. Ferreri, D. Formica, F. Ranieri, M. Tombini, U. Ziemann, J.C. Rothwell, V. Di Lazzaro, Modulation of brain

plasticity in stroke: a novel model for neurorehabilitation, Nat. Rev. Neurol. 10 (10) (2014) 597–608.
[56] Y. Wu, L. Zhong, Z. Yu, J. Qi, Anti-neuroinflammatory effects of tannic acid against lipopolysaccharide-induced BV2 microglial cells via inhibition of NF-κB activation, Drug Dev. Res. 80 (2) (2019) 262–268.
[57] H. Xin, M. Katakowski, F. Wang, J.Y. Qian, X.S. Liu, M.M. Ali, B. Buller, Z. G. Zhang, M. Chopp, MicroRNA-17–92 cluster in exosomes enhance neuroplasticity and functional recovery after stroke in rats, Stroke 48 (3) (2017) 747–753.
[58] B.V. S, Nigel I. Wood, Jenny C. Roberts, Perouz Pambakian, Alan L. Rothaul, A. Jackie Hunter, Tom C. Hamilton, Motor dysfunction in a photothrombotic focal ischaemia model, Behav. Brain Res. 78 (2) (1996) 113–120.
[59] L.Q. Xu, K.G. Neoh, E.T. Kang, Natural polyphenols as versatile platforms for material engineering and surface functionalization, Prog. Polym. Sci. 87 (2018) 165–196.